CHEMICAL ENGINEERING TRANSACTIONS, Volume 11, 2007
Edited by Sauro Pierucci

CFD simulation of a parallel-competitive reaction scheme in an unbaffled vessel

Grisafi Franco, Scargiali Francesca, Brucato Alberto
Dipartimento di Ingegneria Chimica dei Processi e dei Materiali
Viale delle Scienze – 90128 – Palermo (ITALY)

Stirred tanks are widely used in the process industry, often to carry out complex chemical reactions. In many of such cases the perfect mixing hypothesis is not applicable, and more detailed modelling approaches are required in order to accurately describe reactor behaviour. In this work a fully predictive modelling approach, based on Computational Fluid Dynamics, is developed. Model predictions are compared with original experimental data obtained in an unbaffled stirred vessel with parallel-competitive, mixing sensitive reaction scheme. Notably, satisfactory results are obtained with no recourse to micro-mixing models, so highlighting the major role played by macro-mixing in the investigated system.

1. Introduction

In order to avoid the limitations associated with the lumping process and to build-up generally applicable models, distributed parameter modelling of stirred reactors have been developed (Bakker & van den Hakker, 1996; Baldyga & Makowski, 2004). They are based on the actual vessel hydrodynamics and take advantage of the development of commercial codes for computational fluid dynamics (CFD). Micromixing models are often included in the CFD simulations in order to account for unmixedness at scales smaller than the computational grid adopted. In the present work CFD-based simulations of a mixing sensitive homogeneous reaction scheme are carried out and compared with original experimental data. The reactive scheme is that previously adopted by Brucato *et al.* (2000). In that case the experimentation regarded a *baffled* stirred batch reactor and an instantaneous addiction of the common reagent (*A*) at each run start. Results showed that there was no need to resort to micro-mixing models to match simulation and experiment, despite the same reaction scheme had been used in the past to validate micro-mixing models (e.g. Baldyga *et al.*, 1997). In the present work an *unbaffled* tank was used in conjunction with longer injection times.

2. Experimental work

The reactive system employed in this work for the experimentation is the same previously adopted by Brucato *et al.* (2000). It consists of two fast parallel-competitive reactions: the precipitation reaction of cupric hydroxide and the alkaline hydrolysis of ethyl chloroacetate. Both reactions are characterized by second order kinetics but the former is much faster than the latter: at 20°C, the value of k_1 is of the order of 107 $m^3mol^{-1}s^{-1}$ while the kinetic constant k_2 is equal to 0.023 $m^3mol^{-1}s^{-1}$ (Bourne & Yu, 1991).

$$\underset{(A)}{\mathrm{NaOH}} + \underset{(B)}{\tfrac{1}{2}\mathrm{CuSO_4}} \xrightarrow{k_1} \underset{(R1)}{\tfrac{1}{2}\mathrm{Cu(OH)_2}\downarrow} + \underset{(R2)}{\tfrac{1}{2}\mathrm{Na_2SO_4}} \qquad (1)$$

$$\underset{(A)}{\mathrm{NaOH}} + \underset{(C)}{\mathrm{CH_2ClCOOC_2H_5}} \xrightarrow{k_2} \underset{(S1)}{\mathrm{ClCH_2COONa}} + \underset{(S2)}{\mathrm{C_2H_5OH}} \qquad (2)$$

This implies that to all practical purposes reaction (1) can be considered as instantaneous with respect to the reaction (2) when reactant concentrations are of the same order of magnitude. The reaction scheme here employed slightly differs from the well known reaction scheme employed in a number of previous investigations (*e.g.* Bourne & Yu, 1991; Baldyga & Makowski, 2004; Akiti & Armenante, 2004), where the first reaction was the acid-base neutralization of $NaOH$ with HCl. The recourse to the cupric ions in this work lead to easier concentration measurements. In fact, these were simply made by colorimetry, taking advantage of the strong blue coloration of cupric ions. At the same time the problems related to the stoichiometric complexity of the reaction between $Fe3+$ and $OH-$ due to the stability the over-hydroxylated ionic species (Cotton & Wilkinson, 1988) were avoided.

The experimental apparatus consisted of an unbaffled vessel with the inner diameter equal to 0.19 m and closed by a flat lid. A standard radial impeller (Rushton turbine) was used. In all cases an aqueous solution with an initial concentration of 11.5 mol/lt $CuSO_4$ premixed with 21 mol/lt of $CH_2ClCOOC_2H_5$ was utilized. The starting concentration was always checked by withdrawing a small solution sample before starting each run. The operating temperature was kept at 20 °C.

After stable fluid dynamics conditions at a given agitation speed were achieved, a concentrated solution of $NaOH$ (equal to about 1/50 of the tank volume) was fed through a needle (0.5 mm diameter, in order to prevent back-mixing inside the feed tube) placed at an axial position of 3 cm above the vessel bottom. Injection time spanned from few hundreds to several thousand seconds. The apparatus utilised to inject the concentrated $NaOH$ solution consisted of a small reservoir which was suitably filled with the solution and pressurised with air so that a constant flow rate of the co-reactant was injected.

At the end of each injection the total amount of reactant A introduced in the system was such that, in absence of chemical reactions, an average concentration of 21 molt/lt would have been attained. This implies that the amount of A fed would have been just sufficient to digest only one of the two co-reactants B and C previously premixed. The final concentration of reactants, when all the reactant A has disappeared, was determined by measuring the concentration of un-reacted $CuSO_4$ by colorimetry. The selectivity versus reaction 2 was finally computed as follows:

$$Sel = \frac{[C]_{init} - [C]_{final}}{[C]_{init}} \equiv \frac{[B]_{final}}{[B]_{init}} \qquad (3)$$

It is important to observe that, in the case of perfect mixing hypothesis, the final selectivity in all investigated cases should have been of the order of 10^{-8}.

3. CFD modelling

The CFD modelling of the complete reactive system was performed in two separate steps. In the first one the pre-release flow field inside the vessel was simulated. In the second step, while maintaining the same flow field, the two reaction processes were considered by performing fully time-dependent simulations in order to assess the concentration dynamics of reactants. The CFD code utilised was STAR-CD release 3.22 by Adapco. All flow field simulations were performed in the impeller reference frame. With this choice it was possible to carry out steady-state flow field calculations. The system geometry allowed to consider only one sixth of the entire volume (a 60 degrees cylindrical portion). The computational domain which was discretised in $42\times72\times12$ ($r\times z\times\theta$) cells on a cylindrical reference frame. A differential Reynolds Stress second order closure was adopted for turbulence modelling, while the "SIMPLE" algorithm was adopted for the pressure-velocity coupling. The reactive process simulations were performed for all experimental conditions starting from the corresponding steady state flow field. As the injection position did not alter the physical symmetry of the system, in this second step the same computational domain was maintained for the reactions simulations. Due to the low concentration of chemical reacting species their presence did not significantly affect the flow field, therefore they were considered as passive scalars. The injection of reactant A was simulated as a source term in its transport equation, in the cells near the injection point.

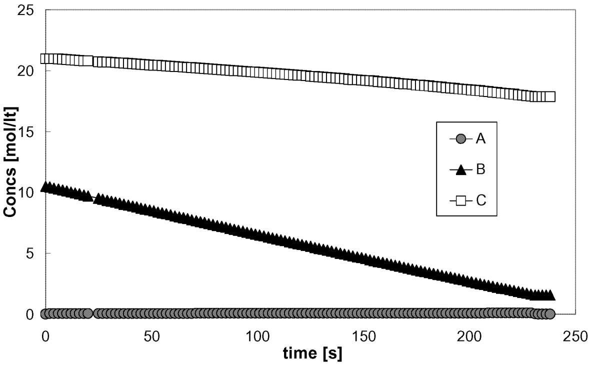

Fig. 1 – Averaged concentration dynamics of reactants (simulation with T_{inj}=230 s, 400 rpm).

Reaction 1 was considered instantaneous: species *A* and *B* were not allowed to co-exist into the same cell. The simulation strategy for the fast reaction consisted of checking the concentrations of reactants *A* and *B* at the beginning of each time step and updating them in such a way that the limiting one disappeared while the concentration of the other one was decreased according to reaction 1 stoichiometry. Reaction 2 was simulated by properly setting the relevant source terms in the transport equations of the two reactants *A* and *C* according to the relevant reaction kinetics. It is worth noting that, in each time step, in the *A* rich locations in the reactor volume the disappearance of *B* due to reaction 1 left in the same cell species *A* and *C*, that were therefore allowed to react according to reaction 2.

A typical simulation result is shown in Fig. 1, in terms of averaged concentration dynamics of all reactants. The observation of Fig. 1 indicates that the average concentrations of reactants *B* and *C* varies almost linearly with time while the concentration of co-reactant *A* is kept roughly constant at values near to zero.

The CPU time required to perform this simulation on a PC equipped with a Pentium 4 running at 2.4 GHz was 240 hours. The extrapolation of CPU time requirement to simulate the longest injection duration (T_{inj}=3445 s) lead to an estimated value of more than 2500 hours which is obviously clearly unviable.

In order to make the simulations affordable also for long injections times, a computational technique which speeds-up concentration dynamics calculations was set up. It is possible to define an average reaction rate $\langle r_i \rangle$ for each reactant as follows:

$$\langle r_i \rangle = \frac{\langle C_i \rangle_{t+dt} - \langle C_i \rangle_t}{dt} \tag{4}$$

where $\langle C_i \rangle_{t+dt}$ and $\langle C_i \rangle_t$ are the averaged (over reactor volume) concentrations of reactant “i” at the generic times t + dt and t respectively. Analysis of the average concentration trends reported for all reactants in Fig. 1 indicates that the average reaction rates tend to become constant few seconds after the injection start. This observation makes it possible to extrapolate the average concentration of reactants *B* and *C* over a macro time interval Δt many times greater than the integration time step, by simply assuming:

$$\langle C_i \rangle_{t+\Delta t} = \langle C_i \rangle_t + \langle r_i \rangle_t \cdot \Delta t \tag{5}$$

where the index “i” may indicate reactant *B* or *C*.

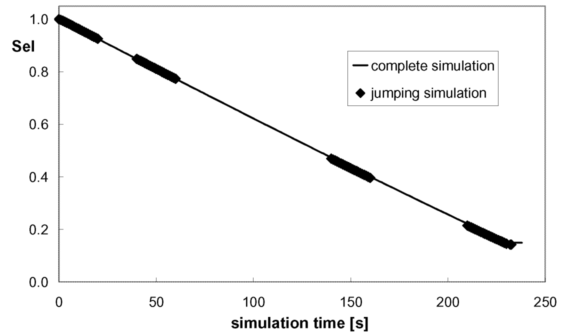

Fig. 2 – Selectivity dynamics, comparison between full and “jumped” sim. results (T_{inj}=230 s, 400 rpm).

In practice, after the average reaction rates stabilise their values, a macro time step Δt is performed by updating the concentration of the generic species “i” into the generic cell “ic” ($C_{i,ic}$) as follows:

$$\left(C_{i,ic}\right)_{t+\Delta t} = \left(C_{i,ic}\right)_t \cdot \langle r_i \rangle_t \cdot \Delta t$$

The common reactant concentration is updated according to the amount introduced during the macro interval and the amount disappeared due to the reactive processes.

In Figure 2 the average selectivity dynamics obtained by performing the simulation with the above described computational “jumping technique” is compared with the relevant value obtained by performing the complete simulation. The very good agreement observed clearly validates the technique. This last was therefore used for all other simulations .

4. Results and discussion

Each simulation was carried out after the injection end until the entire amount of the co-reactant *A* consumed. The final selectivity towards reaction 2 was then computed on the basis of Eq. 3.

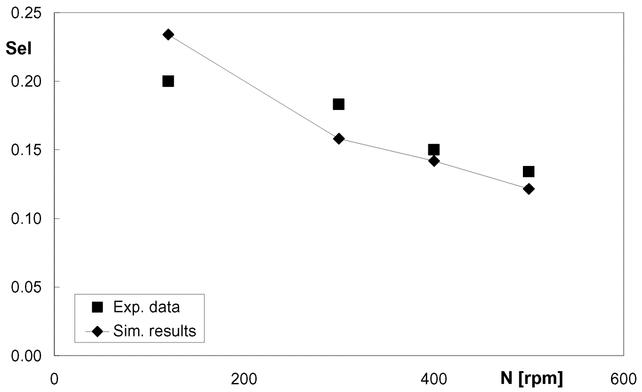

Fig. 3 – Selectivy *vs* agitation speed (T_{inj}=230 s).

The effect of agitation speed on the selectivity towards reaction 2 is shown in Fig. 3. First of all it can be seen the reported values are of the order of 10^{-1}, well above (8 orders of magnitudes!) those predicted under perfect mixing assumption. As mixing intensity increases with agitation speed, a progressive reduction of selectivities is observed. Notably, predicted values are very close to experimental results at all agitation speeds. It is worth stressing that, this good agreement was obtained by taking into consideration only "macro-mixing" phenomena in the tank, though the reactive system employed has been used in a number of works aimed at characterising "micro-mixing" phenomena (e.g. Baldyga *et al.*, 1997; Baldyga & Makowski, 2004).

The effect of the injection time of reactant *A* on the selectivity at constant impeller agitation speed is shown in Figs. 4 and 5, where the results of simulations (diamonds) are compared with experiment at two different agitation speeds. In both cases the selectivity values calculated by the simulations show a favourable agreement with the experimental data. The dependence of selectivity on injection time appears to be well simulated too.

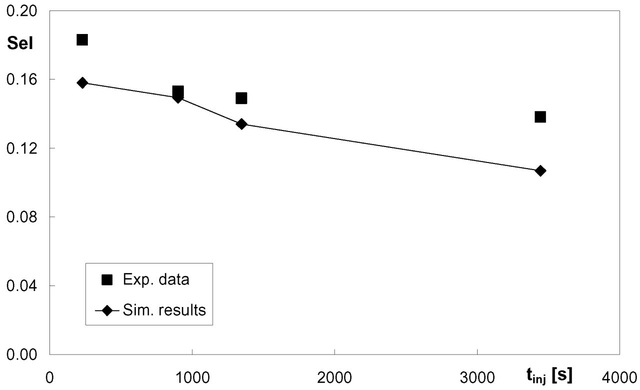

Fig. 4 – Selectivy *vs* injection time (N=300 rpm).

A closer inspection of Figs. 3-5 may indicate that there are minor unresolved effects, possibly due to the micro-mixing phenomena overlooked in the simulations.

In fact the predicted selectivities tend to progressively detach from the experimental values while injection time increases (see Figs. 4 and 5), as if simulations tended to over predict the local mixing intensity. On the other hand, the discrepancies are limited to less than 20% (in the worst case), a figure that can be considered well within the acceptance level for design purposes.

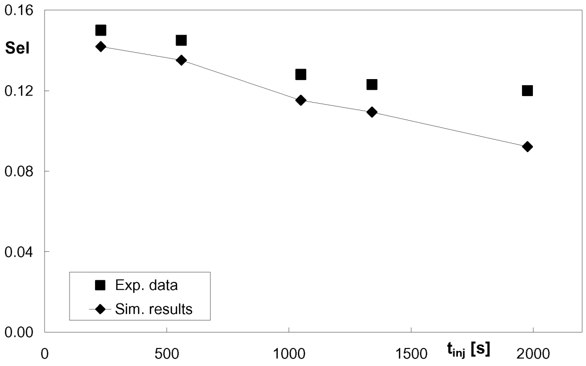

Fig. 5 – Selectivy *vs* injection time (N=400 rpm).

5. Conclusions

A CFD based fully predictive approach was developed to predict the behaviour of a complex reactive system. The computed selectivities were found to agree well with experimental results, although these differed by many orders of magnitude from perfect mixing predictions. As the reaction simulations were performed without considering any sub-grid (micro-mixing) model, it should be concluded that in the investigated case macro-mixing is the main responsible for the reactive behaviour of the system. These findings confirm the similar results obtained by Brucato *et al.* (2000) in the case of instantaneous injectio and baffled vessel.

References

Bakker, R.A., van den Akker, H.E.A., 1996. A lagrangian description of micromixing in a stirred tank reactor using 1D-micromixing models in a CFD flow field, Chemical Engineering Science, 51 (11), 2643-2648.

Baldyga, J., Bourne, J.R., Hearn, S.J., 1997. Interaction between chemical reactions and mixing on various scales, Chemical Engineering Science, 52, 457-466.

Baldyga, J., Makowski, L., 2004. CFD Modelling of mixing effects on the course of parallel chemical reactions carried out in a stirred tank, Chemical Engineering and Technology, 27 (3), 225-231.

Bourne, J.R., Yu, S., 1991. An experimental study of micromixing using two parallel reactions. Proceedings of the 7th European Conference on Mixing, Brugge, Belgium, vol. I, 67–75.

Cotton, F.A., Wilkinson, G., 1988. Advanced inorganic chemistry. 53Ed., New York, Wiley.